Supplemental Information: Medial prefrontal cortex supports perceptual memory

Caspar M. Schwiedrzik, Sandrin S. Sudmann, Thomas Thesen, Xiuyuan Wang, David M. Groppe, Pierre Mégevand, Werner Doyle, Ashesh D. Mehta, Orrin Devinsky and Lucia Melloni

Supplemental Experimental Procedures

Participants

Seven patients undergoing invasive monitoring of pharmacologically resistant epilepsy took part in the study (17-31 yrs old, mean 23.8 yrs, 2 male, 6 right-handed). Demographics and clinical details are provided in Supplementary Table 1. Testing took place at New York University Langone Medical Center (n=6) and at North Shore University Hospital, Manhasset, NY, USA (n=1). Written informed consent was obtained from each participant prior to the experiment, in accordance with the stipulations of the Institutional Review Boards at New York University Langone Medical Center and Feinstein Institute for Medical Research, respectively, and with the Declaration of Helsinki. Patients were aware that taking part in the study would not interfere with their clinical care and that withdrawal was possible at any point without any impact on their clinical care.

Lesion Patient

One of the patients (25 yrs old, female, right-handed) had undergone previous resective surgery for epilepsy (complex partial seizures with secondary generalization) 4 yrs prior to participating in the study. In that surgery, a small resection of part of the left superior frontal gyrus (SFG) was performed. Magnetic resonance imaging (MRI) showed bifrontal and bitemporal craniotomy changes with a resection cavity in the dorsal and medial left frontal lobe and a small

infarct in the left anterior body/genu of the corpus callosum, but no other structural abnormalities (Fig. 1F). The patient was studying towards a master's degree and a neuropsychological examination conducted as part of the clinical care confirmed that the patient was high functioning (Verbal Comprehension (VCI) 117, Perceptual Organization (POI) 102; Wechsler Adult Intelligence Scale).

Stimuli and task

Task and stimuli (Fig. 1A) were similar to a previous study [S1] and are known to elicit robust, orientation-tuned perceptual memory effects [S2]. Subjects were asked to fixate on a red, foveally presented fixation dot. Each trial consisted of two stimuli, presented in succession. First, we presented a bistable, rectangular dot lattice (for 800 ms). This type of stimulus is typically perceived as a collection of lines oriented along one of two orientations, 0°or 90°. By changing the aspect ratio (AR, Δ0/Δ90, where Δ0 and Δ90 correspond to the interdot distances along 0° and 90°) of the dot lattice (possible values: 1.2^{-1}, 1.1^{-1}, 1, 1.1, 1.2), it is possible to manipulate which of two orientations subjects are likely to perceive. Smaller ARs favor 0° percepts; at AR=1, the stimulus is completely bistable. Pseudo randomization assured that each AR occurred equally often. After the first stimulus was presented, participants chose the perceived orientation from a display showing four possible orientations (0°, 90°, and the two diagonal orientations) with a mouse. Second, we presented a tristable, hexagonal dot lattice (for 300 ms). Participants are equally likely to perceive this kind of lattice as oriented along 0°, 60° and 120° if presented in isolation. The first, rectangular, and the second, hexagonal lattice were aligned to the same orientation (henceforth referred to as 0°). This orientation was randomly varied from trial to trial, covering 90° in 1° steps. After presentation of the second lattice, subjects again chose the perceived orientation from a display with four options (0°, 60°, 120°, and the unlikely 90° orientation) with a mouse click. Randomization of the positions of the

answers on the response screens was ensured within and between trails. We also slightly jittered the exact position of the dot lattices (0–1.15°) to prevent that stimuli in successive displays systematically occupied the same space. Finally, a dynamic random dot mask was presented (for 550 ms) to reduce carry-over effects across trials. To separate perceptual from post-perceptual, decisional memory effects, we included a control condition in which no perceptual memory could be formed on the basis of the first stimulus, but subjects nevertheless had to make decisions about orientation. To this end, we replaced the first stimulus with a random dot pattern which did not contain orientation information and thus did not favor the perception of a particular orientation (Supplementary Fig. S1A). Subsequently, participants were asked to decide among four orientations presented on the response screen. Then, as in the main experimental condition, we presented a tristable, hexagonal dot lattice, followed by a response screen. Subjects chose which orientation they perceived in the second stimulus. Last, we presented a dynamic random dot mask. If subjects formed a memory of their decision about orientation in the first stimulus (where no perceptual orientation information was present), we would expect to find a systematic effect of that decision onto the second stimulus, if decisional factors were at play. The main and the control conditions were pseudo-randomly intermixed in blocks of 60 trials. Breaks were self-paced. Patients completed 464 trials on average (82 in the control condition). Stimuli were generated in Matlab (R2007a, The MathWorks). Presentation and response collection were controlled by Presentation software (Neurobehavioral Systems). Stimuli were displayed on a laptop monitor at bedside.

Data acquisition

Data was acquired from a total of 1117 intracranially implanted electrodes. The decision to implant, electrode targeting, and the duration of invasive monitoring were entirely based on clinical considerations and not related to this or any other study. Macroelectrodes were arranged

as grid arrays (8 × 8 contacts, 10 or 5 mm center-to-center spacing), linear strips (1 × 8/12 contacts), or depth electrodes (1 × 8/12 contacts), or some combination thereof.

At New York University Langone Medical Center, signals were acquired with a Nicolet ONE clinical amplifier (Natus), at a sampling rate of 512 Hz, with band pass filtering between 0.5-250 Hz. ECoG signals were online referenced to a screw bolted to the skull. At North Shore University Hospital, signals were acquired with a Brainbox EEG-1166 system (Braintronics) at a sampling rate of 512 Hz and band pass filtered between 0.1-256 Hz and by an XLTEK EMU128FS system (Natus Medical, Pleasanton, California), with a sampling rate of 500 Hz, filtering the signal between 0.07 and 200 Hz. These data were online referenced to a subgaleal electrode at the vertex. All data were stored continuously with stimulus and timing markers permitting offline synchronization.

Surface reconstruction and electrode localization

To localize electrode recording sites, pre-surgical and post-surgical T1-weighted, anatomical MRIs and/or postsurgical high density thin-slice computed tomography (CT) were obtained for the patient and co-registered with each other [S3]. The co-registered images were normalized to the MNI-152 template. A 3-dimensional reconstruction of each patient's brain was computed using FreeSurfer [S4]. Electrode locations were extracted in MNI space (projected to the surface).

Behavior analyses

Behavioral data were analyzed in SPSS (version 24, IBM Corp.) using a logistic regression model in the Generalized Estimating Equations (GEE) framework [S5], as in our previous study [S1]. GEE allows modeling trial-by-trial data while accounting for within-subject and across

trials correlations by defining a first-order, autoregressive 'working correlation matrix'. Data were sorted by subject, block, and trial. We built a regression model with the reported percept of the first stimulus as predictor for the percept of the second stimulus. This model was tested on the group level and per subject. A statistically significant, positive effect of the reported first percept predicting the second percept indicates perceptual memory [S1, 2]. Because perceptual memory does not depend on the AR of the first stimulus [S1, 2], we did not include a separate predictor for AR. Significance of model parameters was assessed using the Wald χ^2 statistic.

To assess whether post-perceptual, purely decisional factors play a role in perceptual memory, we additionally analyzed data from the control condition in which the first stimulus did not contain orientation information. Trials in which subjects chose the 0° orientation in the first stimulus and perceived the 0° orientation in the second stimulus were considered 'decision repetition' trials; trials in which subjects reported one of the remaining three orientations (90° or a diagonal) in the first stimulus and 0° in the second stimulus were considered trials without decision repetition. We then used the non-parametric McNemar test to assess whether decision repetitions occurred more often than chance.

To assess whether the dorsomedial prefrontal cortex (dmPFC) plays a causal role in perceptual memory, we created an additional logistic regression model for all subjects including the data from (and a separate predictor for) the patient with a dmPFC lesion. A significant interaction between the patient predictor and the predictor modelling the percept of the first stimulus indicates that behavior of the lesion patient differed from the non-lesioned patients. In addition, we built a regression model solely for the lesion patient with the percept of the first stimulus as predictor. A non-significant effect of this predictor indicates that the subject does not exhibit perceptual memory.

Electrocorticography analyses - Preprocessing

ECoG data preprocessing was performed in Matlab (R2016a, The Mathworks) using the Fieldtrip toolbox (version 20170327, http://www.fieldtriptoolbox.org) [S6]. Channels were visually inspected and rejected if containing interictal spikes, electromagnetic interferences, and other noticeable signal contaminations, if they lay within the clinically determined seizure onset zone, or if they could not be reliably localized in the MRIs (12% of all channels). We retained 985 artifact-free channels (Supplementary Fig. S1B). Line noise was removed from the signal with notch filters at 60, 120 and 180 Hz), and data were demeaned. For all our main analyses, we focused on the high gamma band (HGB) part of the ECoG signal which has been shown to index the aggregate firing rate [S7, 8]. HGB activity was extracted by band pass filtering between 70 and 150 Hz in 10 Hz wide frequency bands. Subsequently, the envelope on each band pass filtered signal was computed using a standard Hilbert transform. The signal of each band of each channel was normalized (divided) by its mean across the entire recording and transformed to decibel ($10*\log_{10}$). The bands were averaged together to provide a single time series. Where necessary, data were resampled from 512 Hz to 500 Hz using the Piecewise Cubic Hermite Interpolating Polynominal to homogenize sampling rates. The HGB envelope was then segmented from 1 s pre-stimulus until 1 s post-stimulus for the first and second dot lattice, respectively. This time period was then baseline corrected on a trial-by-trial basis [S9]. Specifically, the timepoint-by-timepoint baseline before the first stimulus (-100 until 0 ms) was extracted for each trial, concatenated, and then averaged. This value was then subtracted from each time point in each trial. We also conducted a supplementary analysis of other frequency bands, specifically the theta (4-7 Hz), alpha (8-12 Hz), beta (13-25 Hz), and low gamma (30-50 Hz) bands, following the same procedure as described for the HGB. ECoG data from the lesion patient were not included in the analyses.

Electrocorticography analyses - Regions of interest

Because we were interested in the role of dmPFC in perceptual memory, we focused our analyses on recording sites in the SFG. The SFG makes up most of dmPFC. It is a continuous anatomical region that spans part of the lateral (above the superior frontal sulcus) and most of the medial (up to cingulate sulcus) portions of the anterior frontal lobe. To assess the specificity of perceptual memory effects within PFC, we also selected a control region on the lateral surface of PFC, the rostral middle frontal gyrus (MFG). This region is functionally similar to dmPFC as it has similarly been found to be involved in memory [S10] and contains Brodmann Area 46 [S11], which has been implicated in perceptual decision making [S12]. Electrodes were localized based on FreeSurfer parcellation using the Desikan-Killiany atlas [S13] as well as manual inspection and collapsed across hemispheres. Out of a total of 985 artifact-free recording sites, 180 electrodes were located in our regions of interest (ROIs) (116 in SFG, 64 in MFG). Each patient contributed between 2 and 40 electrodes to the SFG ROI and between 3 and 27 electrodes to the MFG ROI.

Electrocorticography analyses - Identification of visually responsive sites

To isolate recording sites with activity evoked by the dot lattices, we determined the onset latency of each site from the average HGB response to the first stimulus (irrespective of condition) and then determined whether HGB activity was significantly different from the preceding baseline. Onset latency was determined as the first time point after which the average activity in the time window 0-810 ms after stimulus onset exceeded 2 SDs of the mean baseline activity (-50 ms until 0 ms) for at least 50 ms. A two-sided, non-parametric Wilcoxon test was then performed per electrode across trials, comparing the HGB response in the baseline period (-50 ms to 0 ms relative to stimulus 1) with the HGB activity in a 40 ms window starting at the individually determined onset latency. Only electrodes with $p<0.05$ were included in subsequent analyses, irrespective of whether they responded positively or negatively to the

stimulus. For SFG, 102 electrodes (88% of electrodes in SFG) were identified to be visually responsive. For MFG, 61 electrodes (95% of electrodes in MFG) were found to be visually responsive (Fig. 1B). The proportion of positively and negatively responding electrodes was the same in lateral and medial PFC (Fisher Exact Test, p=0.8716), and almost 50-50 (54% of electrodes with a negative response in medial PFC and 56% in lateral PFC). Each patient contributed visually responsive sites in both ROIs, ranging between 2 and 35 electrodes in SFG and between 4 and 26 electrodes in MFG. The average response to the first stimulus is shown in Figure S1C.

Electrocorticography analyses - Statistical analysis

Statistical analyses were carried out in R (version 3.4.3, R Core Team, https://www.R-project.org). To assess whether PFC is involved in perceptual memory, we compared HGB responses (and responses in other frequency bands) to the second dot lattice for the different experimental conditions and ROIs, respectively. 'Perceptual memory' trials were defined as trials in which subjects reported perceiving the main axis (0°) for the first and the second dot lattice. 'No perceptual memory' trials were defined as trials in which subjects reported perceiving any orientation but the main axis for the first stimulus, and the main axis (0°) for the second stimulus. This way, we could compare trials with and without perceptual memory in which subjects had identical percepts (0°). Similarly, we defined 'decisions repetition' trials as trials in which subjects reported twice the same orientation in the control condition, and 'no decision repetition' trials in which they reported two different orientations. For each visually responsive site in SFG and MFG, we calculated the average HGB activity across trials per time point in these four conditions, respectively.

To investigate the time course of neural effects underlying perceptual memory and decision repetition, respectively, we then conducted time-resolved analyses in running average windows

of 150 ms (20 ms steps) from the onset of the second dot lattice until 780 ms post stimulus, followed by correction for multiple comparisons using the false discovery rate (FDR) [S14] at $q<0.05$ with the qvalue package (version 2.10.1, J. D. Storey, A. J. Bass, A. Dabney and D. Robinson, https://github.com/StoreyLab/qvalue).

For group analysis, we implemented linear mixed effects models with subjects as a random effects (intercept) term and electrodes as a nested random effects term using the LME4 package (version 1.1) [S15]. This hierarchical structure of the statistical model captures the hierarchical structure of the data, accounting for differential variability between subjects and within electrodes, and allows for generalization to the population. Models were fitted separately for each time point. Before fitting models, data were aligned and rank-transformed [S16] using the ARTool package (version 0.10.4, M. Kay and J. O. Wobbrock, https://github.com/mjskay/ARTool) to satisfy distributional assumptions. To assess the *anatomical* specificity of effects, we compared 'perceptual memory' with 'no perceptual memory' between SFG and MFG (HGB~condition*roi+(1|subject/electrode)). To assess the *functional* specificity of effects, we compared 'perceptual memory' and 'no perceptual memory' with 'choice repetition' and 'no choice repetition' (HGB~condition*repetition+(1|subject/electrode)). Significance of main effects and interactions was determined using Type III Wald *F*-tests with Kenward-Roger approximation for degrees of freedom with the lmerTest package (version 2.0) [S17]. Post hoc contrasts of least squares means were performed using the lsmeans package (version 2.27) [S18]. Effect size (D_r) and respective 95% CIs were calculated per time window using the square root of the residual variance as the denominator [S19] (Fig. 1C, D, E and Figure S1 E, F). In addition, we computed default Bayes factors via Gaussian quadrature [S20] for post hoc contrasts using the BayesFactor package (version 0.9.12, R. D. Morey and J. N. Rouder, https://cran.r-project.org/package=BayesFactor).

The same procedures were followed to analyze responses in other frequency bands and to the first stimuli in the trial. To assure that these analyses of the first stimuli were not affected by selection bias, we performed them without pre-selecting visually responsive electrodes on the basis of the first stimulus, and instead analyzed all electrodes within the anatomically defined SFG and MFG ROIs. To avoid any confounds on the level of the stimulus or percept, we re-sorted the trials into "future perceptual memory" trials, where subjects perceived the same (0°) orientation in the first and the second stimulus, and "no future perceptual memory" trials, where subjects perceived 0° in the first but not the second stimulus. This allowed us to compare trials with identical stimuli and percepts for the first stimulus, which only differed in whether they would later result in perceptual memory or not.

Supplemental Table S1

Patient ID		**LIJ085**	**NY359**	**NY386**	**NY507**	**NY536**	**NY628**	**NY383 (lesion patient)**
Gender		F	F	F	F	M	M	F
Age		20	17	20	24	30	31	25
Handedness		R	R	L	R	R	R	R
Implanted hemisphere		L/R	R	L/R	L	L/R	L/R	L
Number of electrodes		324	113	97	83	97	180	
WAIS	**VCI**		89	112	79	127		117
	PRI (POI)		102	98	89	109		102
	WMI		104	105		86		
	PSI		112	92		105		
Language lateralization		N/A	N/A	L	L	N/A	L	N/A
Seizure type		CPS	CPS	CPS	CPS, SGE	CPS	CPS	CPS, SGE
Age of onset		11	5	6	17	7	15	4

Neuropsychological assessments are shown for Wechsler Adult Intelligence Scale (WAIS) subscores Verbal Comprehension Index (VCI), Perceptual Reasoning Index (PRI), Perceptual Organization Index (POI), Working Memory Index (WMI), and Processing Speed Index (PSI). Abbreviations denote: Female (F), Male (M), Left (L), Right (R), not available (N/A), Complex Partial Seizure (CPS), Secondary Generalization (SGE). Language lateralization was assessed in a subset of patients using the intracarotid sodium amobarbital procedure [S21].

Supplemental Figure S1

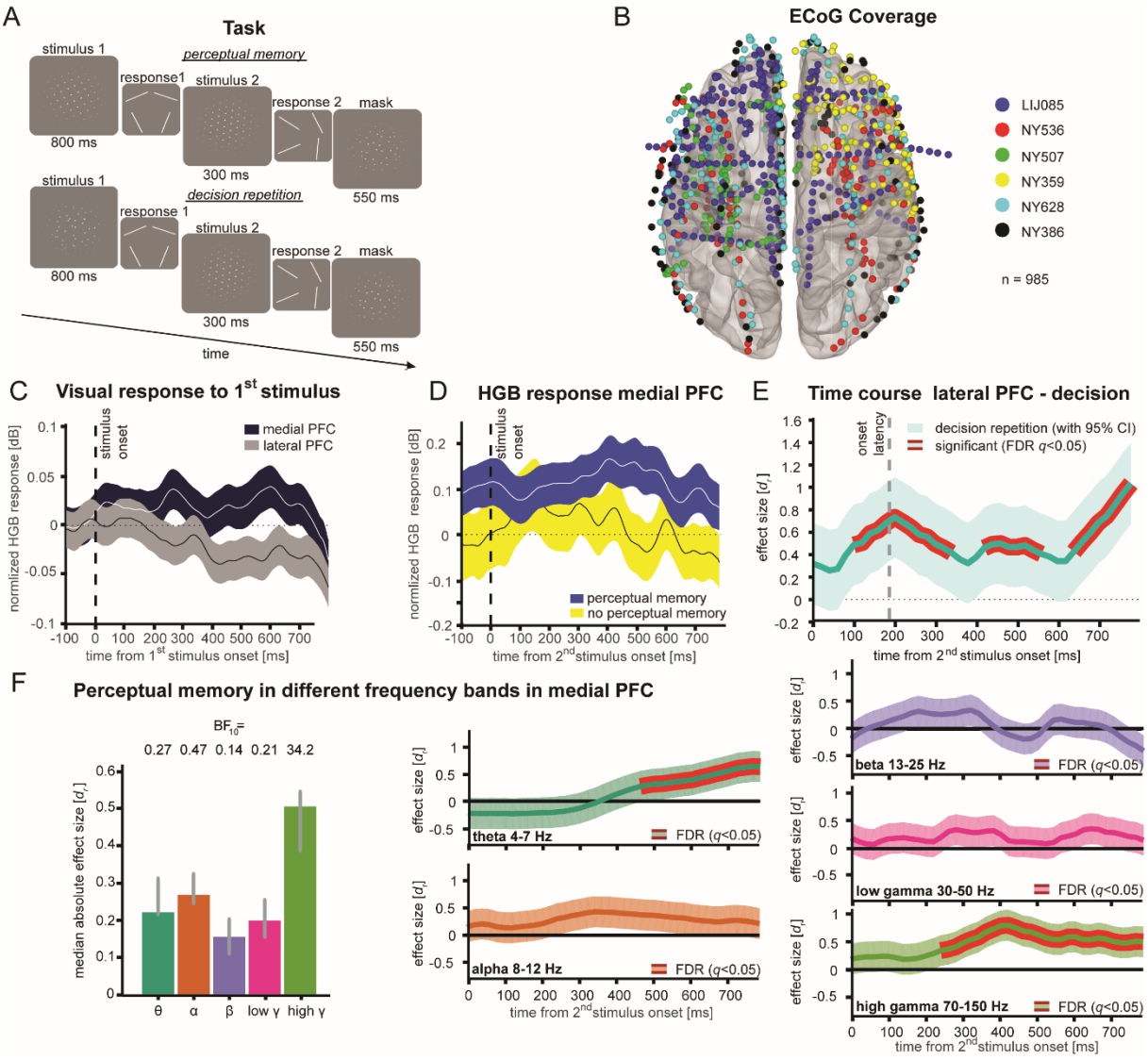

Figure S1: **(A)** To distinguish perceptual from decisional memory effects, subjects were asked to make decisions about orientation in the absence of orientation information (stimulus 1, lower panel) on a subset of trials. We then presented the same tristable hexagonal dot lattices as in the main experiment (stimulus 2) to assess whether prior decisions alone, in the absence of sensory information, affected orientation perception. Carry-over effects between trials were avoided by use of a dynamic random dot mask at the end of each trial. **(B)** We recorded from a total of 985 artifact-free surface and depth electrodes across six patients. Electrode locations are shown on the MNI-152 template. The color code denotes individual subjects. **(C)** Normalized HGB responses to the first stimulus, independent of conditions, from electrodes located in our ROIs.

Shading indicates the standard error of the mean (SEM). **(D)** HGB response of visually responsive electrodes in the medial PFC in trials with perceptual memory (blue) and trials without perceptual memory (yellow). Shading indicates SEM. **(E)** Time course of effect size (D_r) for decision memory in lateral PFC. Note that there were no significant behavioral effects. Shading indicates 95% CIs of effect size (D_r). **(F)** Activity in the theta (4-7Hz), alpha (8-12Hz), beta (13-25Hz), low gamma (30-50Hz) and high gamma (70-150Hz) frequency bands was investigated separately. The absolute effect size (left panel), as well as the time courses for each frequency band (right panel), reveal most prominent perceptual memory effects in the HGB (median D_r=0.51, median BF_{10}=34.2), and a smaller effect in the theta band (median D_r=0.22, median BF_{10}=0.27). Error bars (left) denote bootstrapped 95% CIs, shading (right) indicates parametric 95% CIs of effect size.

Supplemental References

S1. Schwiedrzik, C.M., Ruff, C.C., Lazar, A., Leitner, F.C., Singer, W., and Melloni, L. (2014). Untangling perceptual memory: hysteresis and adaptation map into separate cortical networks. Cereb. Cortex *24*, 1152-1164.

S2. Gepshtein, S., and Kubovy, M. (2005). Stability and change in perception: spatial organization in temporal context. Exp. Brain. Res. *160*, 487-495.

S3. Yang, A.I., Wang, X., Doyle, W.K., Halgren, E., Carlson, C., Belcher, T.L., Cash, S.S., Devinsky, O., and Thesen, T. (2012). Localization of dense intracranial electrode arrays using magnetic resonance imaging. Neuroimage *63*, 157-165.

S4. Fischl, B. (2012). FreeSurfer. Neuroimage *62*, 774-781.

S5. Liang, K.-Y., and Zeger, S.L. (1986). Longitudinal data analysis using generalized linear models. Biometrika *73*, 13-22.

S6. Oostenveld, R., Fries, P., Maris, E., and Schoffelen, J.M. (2011). FieldTrip: Open source software for advanced analysis of MEG, EEG, and invasive electrophysiological data. Comput. Intell. Neurosci. *2011*, 156869.

S7. Ray, S., Crone, N.E., Niebur, E., Franaszczuk, P.J., and Hsiao, S.S. (2008). Neural correlates of high-gamma oscillations (60-200 Hz) in macaque local field potentials and their potential implications in electrocorticography. J. Neurosci. *28*, 11526-11536.

S8. Manning, J.R., Jacobs, J., Fried, I., and Kahana, M.J. (2009). Broadband shifts in local field potential power spectra are correlated with single-neuron spiking in humans. J. Neurosci. *29*, 13613-13620.

S9. Ciuparu, A., and Muresan, R.C. (2016). Sources of bias in single-trial normalization procedures. Eur. J. Neurosci. *43*, 861-869.

S10. Wager, T.D., and Smith, E.E. (2003). Neuroimaging studies of working memory: a meta-analysis. Cogn. Affect. Behav. Neurosci. *3*, 255-274.

S11. Kikinis, Z., Fallon, J.H., Niznikiewicz, M., Nestor, P., Davidson, C., Bobrow, L., Pelavin, P.E., Fischl, B., Yendiki, A., McCarley, R.W., et al. (2010). Gray matter volume reduction in rostral middle frontal gyrus in patients with chronic schizophrenia. Schizophr. Res. *123*, 153-159.

S12. Heekeren, H.R., Marrett, S., and Ungerleider, L.G. (2008). The neural systems that mediate human perceptual decision making. Nat. Rev. Neurosci. *9*, 467-479.

S13. Desikan, R.S., Segonne, F., Fischl, B., Quinn, B.T., Dickerson, B.C., Blacker, D., Buckner, R.L., Dale, A.M., Maguire, R.P., Hyman, B.T., et al. (2006). An automated labeling system for subdividing the human cerebral cortex on MRI scans into gyral based regions of interest. Neuroimage *31*, 968-980.

S14. Storey, J.D., Taylor, J.E., and Siegmund, D. (2004). Strong control, conservative point estimation and simultaneous conservative consistency of false discovery rates: a unified approach. J. Roy. Stat. Soc. B *66*, 187-205.

S15. Bates, D., Maechler, M., Bolker, B., and Walker, S. (2015). Fitting linear mixed-effects models using lme4. J. Stat. Software *67*, 1-48.

S16. Higgins, J.J., and Tashtoush, S. (1994). An aligned rank transform test for interaction. Nonlinear World *1*, 201-211.

S17. Kuznetsova, A., Brockhoff, P.B., and Christensen, R.H.B. (2017). lmerTest package: tests in linear mixed effects models. J. Stat. Software *82*, 1-26.

S18. Lenth, R.V. (2016). Least-squares means: the R package lsmeans. J. Stat. Software *69*, 1-33.

S19. Rouder, J.N., Morey, R.D., Speckman, P.L., and Province, J.M. (2012). Default Bayes factors for ANOVA designs. J. Math. Psychol. *56*, 356-374.

S20. Rouder, J.N., Speckman, P.L., Sun, D., Morey, R.D., and Iverson, G. (2009). Bayesian t tests for accepting and rejecting the null hypothesis. Psychon. Bull. Rev. *16*, 225-237.

S21. Wada, J., and Rasmussen, T. (1960). Intracarotid injection of sodium amytal for the lateralization of cerebral speech dominance J. Neurosurg. *17*, 266-282.